Electronic Supplementary Material (ESI) for CrystEngComm
This journal is © The Royal Society of Chemistry 2012

-Supplementary information file-

The low-/room-temperature forms of the lithiated salt of 3,6-dihydroxy-2,5-dimethoxy-p-benzoquinone: a combined experimental and dispersion-corrected density functional study

Gaëtan Bonnard,[a] Anne-Lise Barrès,[a,b] Olivier Mentré,[c] Damian G. Allis,[d] Carlo Gatti,[e]

Philippe Poizot[a] and Christine Frayret[a]*

[a] *Laboratoire de Réactivité et Chimie des Solides - UMR CNRS 7314, Institut de Chimie de Picardie - FR 3085 CNRS, Université de Picardie Jules Verne, 33, rue Saint-Leu, 80039 Amiens cedex (France)*

[b] *Laboratoire des Glucides - FRE CNRS 3517, Institut de Chimie de Picardie - FR 3085 CNRS, Université de Picardie Jules Verne, 33, rue Saint-Leu, 80039 Amiens cedex (France)*

[c] *Unité de Catalyse et de Chimie du Solide, équipe de Chimie du Solide - UMR CNRS 8181, ENSC Lille-UST Lille, Cité Scientifique - Bât. C7 - BP 80108, 59655 Villeneuve d'Ascq cedex (France)*

[d] *Department of Chemistry, Syracuse University, Syracuse, NY 13244, United States*

[e] *CNR-ISTM, Istituto di Scienze e Tecnologie Molecolari, via Golgi 19, 20133, Milano, Italy*

Contents

1. Thermal analysis

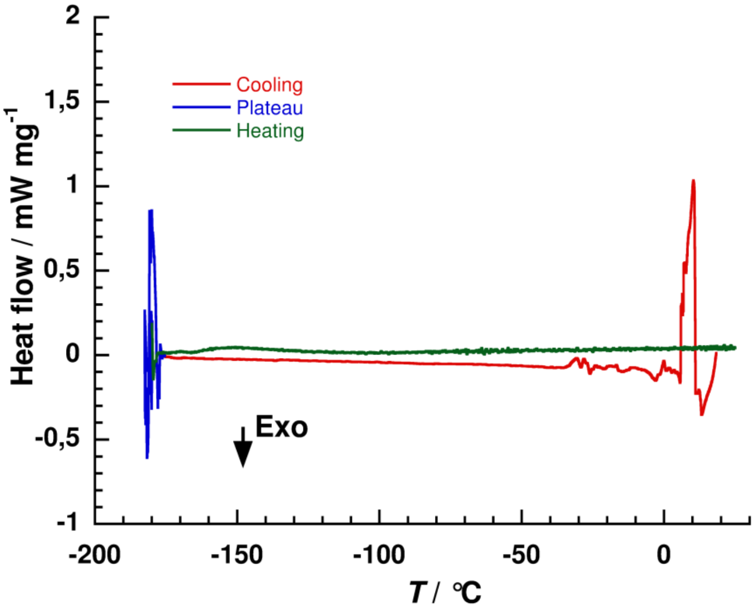

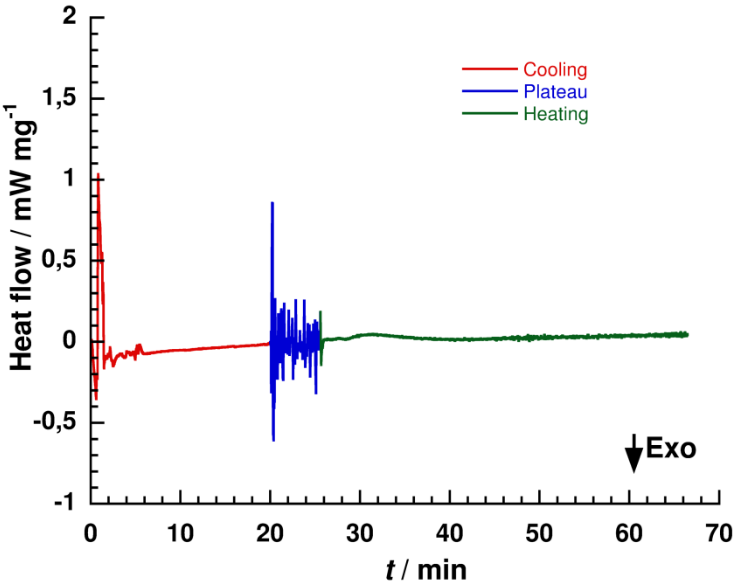

Fig. S1. DSC analysis measurement showing no thermal event upon cooling and heating, as well as during the plateau at 93 K.

The sample was cooled down to 93 K and kept at that temperature for 5 min to stabilize the base measurement, and then was heated up to 25°C at 5 K.min^{-1}. Upon one cooling-heating cycle (RT - 93 K) with a plateau at 93 K for several minutes to stabilize, no specific thermal event occurred, *i.e.* no phase transition is expected. The first peaks at the beginning of the experiment are due to thermal resistance of the furnace and other peaks emerging at the beginning and at the end of the plateau can be ascribed to an artifact from the apparatus relative to rate and temperature changes.

2. X-ray crystallographic data

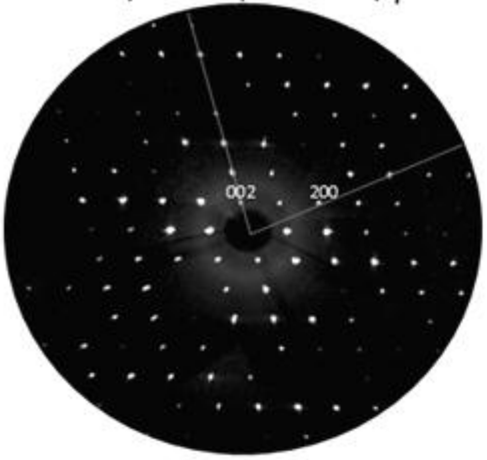

a) T=293K ($P2_1/n$)
a=5.34 ,b=9.53, c=12.79, β = 96.54°

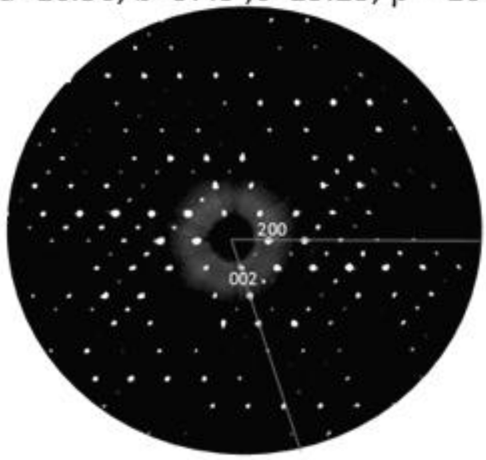

b) T= 100 K ($P2_1/n$)
a=10.56, b=9.49 ,c=13.23, β = 107.93°

Fig. S2. The (h0l) layer precession frame calculated from single crystal data collection at room temperature (a) and 100 K (b). The supercell spots are evidenced in the latter. The blue lines indicate a* and c* directions.

3. Computational details

In the VASP calculations based on a plane wave basis set, we employed projector augmented-wave pseudopotentials (PAW)[1] in which the semi-core states are treated as valence. An energy cut-off of 520 eV was applied. The Brillouin zone sampling was performed using the Monkhorst-Pack scheme[2] with a k-points grid of 4x2x2. The structure was fully relaxed with the threshold of 10^{-5} eV for energy convergence and 10^{-3} eV/Å for residual forces. In order to take into account dispersion forces, we have employed a semi-empirical method developed by Grimme[3] that includes the long-range contributions via damped pairwise $f_{dmp}(R)C_6R^{-6}$ terms at a negligible cost compared to standard

DFT calculations (see [4,5]). The damping function $f_{dmp}(R)$ must be used to avoid near-singularities for small R values and double-counting effects of correlation at intermediate distance:

$$f_{dmp}(R) = \frac{1}{1+e^{-d(R/R_r-1)}} \quad \text{where } R_r \text{ is the sum of atomic vdW radii, } R_{vdW.} \tag{1}$$

Such dispersion corrections are introduced as:

$$E_{disp} = -s_6 \sum_{i=1}^{N-1} \sum_{j=i+1}^{N} \sum_{g} \frac{C_6^{ij}}{R_{ij,g}^6} f_{dmp}\left(R_{ij,g}\right) \tag{2}$$

where the energy is the summation over all atom pairs and *g* lattice vectors, *N* is the number of atoms, s_6 is a functional-dependent global scaling factor, C_6^{ij} is the dispersion coefficient of atom pair *ij*, and $R_{ij,g}$ is the inter-nuclear separation of the atom pair. This treatment applied to the PBE functional and thus labeled PBE-D has gained popularity, providing an improved description of molecular systems. However, Civalleri *et al.*[6,7] demonstrated the need to adjust the parameterization (from PBE-D to PBE-D*) for the application of the method to crystalline solids. For PBE-D* parameterization[6], R_r is multiplied by 1.3 for H and by 1.05 for the other atoms. In previous works,[4,5] we observed a better agreement between optimized geometry using this method and experimental structures of lithiated organic crystals, although no complete transferability of the modified set was reached. In addition to the vdW radii modification, the s_6 value should also be adjusted in some cases.[4] Especially, for the study of the β-phase, we performed a screening of the s_6 parameter within the range: 0.75 - 0.52. Within this set, the method labeled corr-PBE-D*_0.52, corresponding to the s_6 value 0.52 (instead of 0.75 used for PBE-D/PBE-D*) and to the concomitant vdW radii modification of PBE-D* was identified as the most optimized treatment for this phase. In the present study, we tried to see if a further decrease of the s_6 value for this phase at RT could improve its geometry optimization. An improvement was indeed found for the s_6 value of 0.36 concerning the β-form, therefore leading us to consider the corr-PBE-D*_0.36 method. On the other hand for the treatment of the α-phase, the $s_6 = 0.52$ value (corresponding to the corr-PBE-D*_0.52 calculations) was clearly identified as providing the best agreement among the various tested methods.

The all-electron code CRYSTAL09,[8,9] relying on first principles DFT-LCAO instead of using plane waves was also employed by taking the hybrid functional B3PW91[10] with the 6-31G(d,p) Gaussian-type basis set[11-13] within the DFT-D treatment of Grimme. The SCF convergence threshold on the total energy was fixed at 10^{-12} Ha and the optimization convergence criterion on the RMS of the displacement at 10^{-3} eV/Å. Truncation criteria for bielectronic integrals (Coulomb and HF exchange series) were set to 10^{-7}, 10^{-7}, 10^{-7}, 10^{-7} and 10^{-14} Hartree. 104101 and 207621 total grid points were used for the β– and α-polymorph structures, respectively. A pruned (55,434) integration grid was used for the radial and angular distribution of grid points.

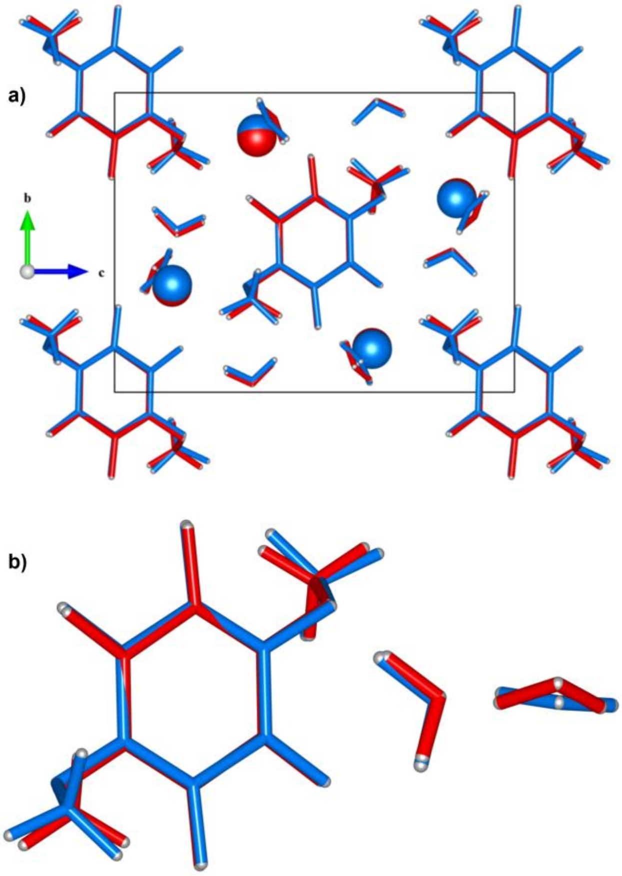

Fig. S3. a) Overlay of the β-phase for the structure at RT (red) and the minimized structure by using the corr-B3PW91-D*_0.36 method (blue) viewed down the *a* axis. b) Zoom in the overlay of the Li_2DHDMQ^{2-} anion and water molecules.

Table S1. Theoretically and experimentally determined intramolecular bond distances for the polymorphic α–form.

	EXP	Theoretical calculation		
	100K	PBE-D*	corr-PBE-D*_0.52	corr-B3PW91-D*_0.52
d(C-C)				
d(C_{1a}-C_{2a})	1.387(1)	1.401	1.399	1.396
d(C_{2a}-C_{3a})	1.411(1)	1.414	1.412	1.412
d(C_{3a}-C_{1a})	1.533(1)	1.533	1.535	1.532
d(C_{1b}-C_{2b})	1.402(1)	1.411	1.413	1.408
d(C_{2b}-C_{3b})	1.394(1)	1.402	1.405	1.399
d(C_{3b}-C_{1b})	1.537(1)	1.534	1.532	1.533
<*d*(C-C)>	**1.444**	**1.449**	**1.449**	**1.447**
<*d*(C-C) except (C3-C1) >	**1.399**	**1.407**	**1.407**	**1.404**
<*d*(C3-C1)>	**1.535**	**1.534**	**1.534**	**1.533**
d(C-O)				
d(C_{4a}-O_{2a})	1.436(1)	1.448	1.446	1.431
d(C_{1a}-O_{1a})	1.271(1)	1.279	1.281	1.268
d(C_{2a}-O_{2a})	1.392(1)	1.388	1.392	1.378
d(C_{3a}-O_{3a})	1.252(1)	1.265	1.267	1.253
d(C_{4b}-O_{2b})	1.440(1)	1.448	1.451	1.453
d(C_{1b}-O_{1b})	1.257(1)	1.267	1.266	1.255
d(C_{2b}-O_{2b})	1.393(1)	1.391	1.388	1.381
d(C_{3b}-O_{3b})	1.263(1)	1.275	1.273	1.262
<*d*(C-O)>	**1.338**	**1.345**	**1.346**	**1.335**
<*d*(delocalized C-O)>	**1.261**	**1.272**	**1.272**	**1.260**
RMSD C-C , C-O		0.009	0.009	0.007
d(C-H)				
d(C_{4a}-H_{1a})	0.99(1)	1.099	1.099	1.090
d(C_{4a}-H_{2a})	0.96(1)	1.097	1.097	1.092
d(C_{4a}-H_{3a})	0.98(1)	1.096	1.096	1.094
d(C_{4b}-H_{1b})	0.99(1)	1.099	1.099	1.094
d(C_{4b}-H_{2b})	0.97(1)	1.099	1.099	1.093
d(C_{4b}-H_{3b})	0.96(2)	1.096	1.095	1.090
<*d*(C-H)>	**0.98**	**1.098**	**1.098**	**1.092**
d(O-H)				
d(O_{W1}-H_{W1a})	0.85(1)	0.999	0.998	0.986
d(O_{W1}-H_{W1b})	0.84(1)	0.996	0.998	0.989
d(O_{W2}-H_{W2a})	0.80(1)	0.989	0.99	0.978
d(O_{W2}-H_{W2b})	0.80(1)	0.992	0.992	0.980
d(O_{W3}-H_{W3a})	0.83(1)	0.993	0.995	0.981
d(O_{W3}-H_{W3b})	0.86(2)	1.007	1.005	0.993
d(O_{W4}-H_{W4a})	0.80(1)	1.009	1.009	0.991
<*d*(O-H)>	**0.83**	**0.996**	**0.997**	**0.984**

Table S2. Experimental and optimized lattice parameters, *a*, *b*, *c* and *β*, unit cell volume *V*, and inter-plane distance, *d*. Numbers between brackets correspond to instrumental error for experimental results and discrepancies with the experiment for theoretical data.

		a (Å)	*b* (Å)	*c* (Å)	*β* (°)	*V/Z* (Å^3)	*d* (Å)
β-phase	Exp.	5.3318(5)	9.5162(9)	12.781(1)	96.493(1)	322.2(1)	4.66
	PBE-D*	5.1390 (-3.6%)	9.5921 (+0.7%)	12.7964 (+0.2%)	96.739 (+0.3%)	313.215 (-1.4%)	4.54 (-2.1%)
	corr-PBE-D*_0.36	5.1882 (-2.7%)	9.6447 (+1.4%)	13.0143 (+1.8%)	98.296 (+1.9%)	322.2 (+0.0%)	4.66 (+0.0%)
	corr-PBE-D*_0.52	5.1561 (-3.2%)	9.6096 (+0.9%)	12.9829 (+1.6%)	97.866 (+1.4%)	318.6 (-0.6%)	4.62 (-0.9%)
	corr-B3PW91-D*_0.36	5.1825 (-2.8%)	9.5773 (+0.6%)	13.0395 (+2.02%)	98.219 (+1.78%)	320.28 (-0.3%)	4.71 (+1.1%)
α-phase	Exp.	10.5610(8)	9.4941(7)	13.2344(8)	107.394(3)	316.6(1)	4.61
	PBE-D*	10.4202 (-1.3%)	9.6085 (+1.3%)	13.0551 (-1.3%)	107.335 (-0.1%)	311.94 (-1.5%)	4.52 (-2.0)
	corr-PBE-D*_0.52	10.4847 (-0.75)	9.6295 (+1.5%)	13.0958 (-1.0%)	106.527 (-0.8%)	316.89 (-0.0%)	4.59 (-0.4%)
	B3PW91-D*_0.52	10.4836 (-0.7%)	9.4490 (-0.5%)	13.2521 (+0.13%)	106.616 (-0.7%)	314.48 (-0.7%)	4.65 (+0.9%)

Table S3. AIM analysis a) of the α-phase (at the corr-B3PW91-D*_0.52 level of theory); b) of the β-phase (at the corr-B3PW91-D*_0.36 level of theory). Calculated interatomic distance, $R_{A\text{-}B}$, electron density at BCP, $\rho(r_C)$, Laplacian of electron density at BCP, $\nabla^2\rho(r_C)$, Eigenvalues λ_1, λ_2 and λ_3 of hessian of electron density, $|\lambda_1|/\lambda_3$ ratio and Bond Ellipticity, ε.

a)

	$R_{A\text{-}B}$ (Å)	**$\rho(r_C)$ (e.Å^{-3})**	**$\nabla^2\rho(r_C)$ (e.Å^{-5})**	**λ_1 (e.Å^{-5})**	**λ_2 (e.Å^{-5})**	**λ_3 (e.Å^{-5})**	**$\lvert\lambda_1\rvert/\lambda_3$**	**ε**
C-C								
C_{3a}-C_{2a}	1.412	2.085	-20.509	-16.098	-12.434	8.024	2.006	0.29
C_{3a}-C_{1a}	1.532	1.714	-14.820	-12.409	-11.470	9.060	1.370	0.08
C_{2a}-C_{1a}	1.396	2.139	-21.401	-16.652	-12.484	7.760	2.146	0.33
C_{3b}-C_{2b}	1.399	2.126	-21.159	-16.509	-12.434	7.806	2.114	0.33
C_{3b}-C_{1b}	1.533	1.714	-14.820	-12.409	-11.470	9.060	1.370	0.08
C_{2b}-C_{1b}	1.408	2.099	-20.651	-16.195	-12.388	7.928	2.043	0.31
C-O								
C_{3a}-O_{3a}	1.253	2.490	2.193	-21.305	-21.255	44.753	0.476	0.00
C_{2a}-O_{2a}	1.378	1.869	-7.785	-12.820	-12.170	17.205	0.745	0.06
C_{1a}-O_{1a}	1.268	2.423	-1.132	-20.341	-20.123	39.328	0.517	0.01
C_{4a}-O_{2a}	1.431	1.653	-8.988	-10.170	-9.928	11.085	0.917	0.02
C_{3b}-O_{3b}	1.262	2.443	0.386	-20.605	-20.555	41.546	0.496	0.00
C_{2b}-O_{2b}	1.381	1.856	-7.135	-12.602	-11.856	17.327	0.727	0.06
C_{1b}-O_{1b}	1.255	2.477	1.686	-21.112	-20.966	43.763	0.482	0.01
C_{4b}-O_{2b}	1.433	1.647	-9.060	-10.120	-9.810	10.845	0.933	0.03
C-H								
C_{4a}-H_{1a}	1.090	1.937	-25.351	-18.916	-18.073	11.638	1.625	0.05
C_{4a}-H_{2a}	1.092	1.930	-24.990	-18.773	-17.905	11.663	1.610	0.05
C_{4a}-H_{3a}	1.090	1.917	-24.605	-18.555	-17.712	11.663	1.591	0.05
C_{4b}-H_{1b}	1.094	1.923	-24.630	-18.580	-17.712	11.663	1.593	0.05
C_{4b}-H_{2b}	1.093	1.930	-25.137	-18.798	-17.977	11.617	1.618	0.05
C_{4b}-H_{3b}	1.090	1.937	-25.351	-18.895	-18.052	11.617	1.627	0.05
O-H								
O_{W1}-H_{W1a}	0.989	2.234	-46.295	-41.956	-41.185	36.846	1.139	0.02
O_{W1}-H_{W1b}	0.986	2.261	-47.138	-42.464	-41.692	37.014	1.147	0.02
O_{W2}-H_{W2a}	0.981	2.301	-48.366	-43.331	-42.439	37.378	1.159	0.02
O_{W2}-H_{W2b}	0.978	2.321	-48.366	-43.378	-42.439	37.475	1.158	0.02
O_{W3}-H_{W3a}	0.993	2.193	-45.449	-41.424	-40.678	36.653	1.130	0.02
O_{W3}-H_{W3b}	0.981	2.294	-48.270	-43.160	-42.389	37.282	1.158	0.02
O_{W4}-H_{W4a}	0.991	2.234	-46.295	-41.810	-41.039	36.557	1.144	0.02
O_{W4}-H_{W4b}	0.976	2.348	-49.281	-43.860	-43.017	37.593	1.167	0.02
O···H-C^{methyl}								
O_{W2}···H_{2b}-C_{4b} (HB1)	2.730	0.040	0.482	-0.121	-0.096	0.721	0.167	0.21
O_{3a}···H_{3b}-C_{4b} (HB2)	2.524	0.061	0.843	-0.193	-0.168	1.203	0.160	0.16
O_{3b}···H_{1a}-C_{4a} (HB3)	2.712	0.047	0.650	-0.121	-0.071	0.843	0.143	0.55
O_{W4}···H_{2a}-C_{4a} (HB4)	2.801	0.034	0.507	-0.096	-0.046	0.650	0.148	1.06
O_{W3}···H_{3b}-C_{4b} (HB5)	2.985	0.027	0.386	-0.071	-0.046	0.507	0.143	0.23
O_{W4}···H_{2b}-C_{4b} (HB6)	2.978	0.027	0.361	-0.071	-0.025	0.457	0.158	1.33
O_{W2}···H_{2a}-C_{4a} (HB7)	2.885	0.027	0.386	-0.071	-0.071	0.554	0.130	0.26
O-H···$C^{carbonyl}$								
O_{W3}-H_{W3b}···C_{1a} (HB8)	2.642	0.223	2.289	-1.132	-1.107	4.532	0.250	0.04

O_{W4}-H_{W4b}···C_{1a} (HB9)	2.662	0.196	2.096	-0.939	-0.893	3.953	0.238	0.05
C-H···C								
C_{4b}-H_{1b}···C_{2a} (HB10)	2.788	0.047	0.507	-0.143	-0.096	0.771	0.188	0.49
C_{4a}-H_{3a}···C_{2b} (HB11)	2.838	0.047	0.507	-0.143	-0.071	0.700	0.207	0.98
O···H–O								
O_{1a}···H_{W3b}-$O_{W3'}$ (HB11)	1.827	0.223	2.289	-1.132	-1.107	4.532	0.250	0.04
O_{1a}···H_{W4b}-$O_{W4'}$ (HB12)	1.871	0.196	2.096	-0.939	-0.893	3.953	0.238	0.05
O_{3a}···H_{W1a}-O_{W1} (HB13)	1.707	0.290	3.132	-1.711	-1.686	6.531	0.262	0.03
O_{W3}···H_{W4a}-O_{W4} (HB14)	1.732	0.283	3.060	-1.614	-1.543	6.192	0.261	0.05
O_{W1}···H_{W2a}-O_{W2} (HB15)	1.797	0.236	2.532	-1.278	-1.203	5.035	0.254	0.06
O_{W4}···H_{W2b}-O_{W2} (HB16)	1.812	0.243	2.435	-1.253	-1.228	4.939	0.254	0.02
O_{3b}···H_{W3a}-O_{W2} (HB17)	1.673	0.317	3.350	-1.928	-1.878	7.156	0.269	0.02
Li···O								
Li_2···O_{1a}	2.228	0.094	2.000	-0.457	-0.361	2.796	0.164	0.27
Li_2···O_{3a}	2.067	0.135	3.157	-0.746	-0.721	4.628	0.161	0.03
Li_2···O_{W3}	2.086	0.135	3.035	-0.771	-0.746	4.532	0.170	0.04
Li_1···O_{1b}	2.054	0.142	3.350	-0.796	-0.721	4.867	0.163	0.09
Li_1···O_{W1}	1.986	0.175	4.192	-1.086	-1.036	6.289	0.172	0.04
Li_1···O_{W4}	2.000	0.155	3.975	-0.939	-0.893	5.807	0.162	0.04
Li_1···O_{3b}	2.020	0.155	3.735	-0.893	-0.843	5.471	0.163	0.04
Li_2···O_{W2}	1.921	0.189	5.110	-1.253	-1.132	7.496	0.167	0.09
Li_2···O_{2b}	2.227	0.081	1.903	-0.432	-0.361	2.725	0.159	0.23
Li···C								
Li_2···C_{3a}	2.894	0.135	3.157	-0.746	-0.721	4.628	0.161	0.03
Li_1···C_{3b}	2.800	0.155	3.735	-0.893	-0.843	5.471	0.163	0.04
O···O								
O_{3a}···O_{2b}	2.837	0.074	0.914	-0.218	-0.168	1.300	0.167	0.18
O_{W3}···O_{3b}	2.666	0.317	3.350	-1.928	-1.878	7.156	0.269	0.02
O_{W3}···O_{2b}	2.957	0.067	0.818	-0.193	-0.143	1.182	0.163	0.44
O_{1b}···O_{W1}	2.700	0.270	2.939	-1.518	-1.471	5.953	0.255	0.03
O_{2a}···O_{W1}	2.878	0.074	1.011	-0.218	-0.143	1.375	0.158	0.62
O_{3b}···O_{2a}	2.912	0.061	0.796	-0.193	-0.143	1.132	0.170	0.21
H···H								
H_{2a}···H_{W4b}	2.358	0.034	0.507	-0.096	-0.046	0.650	0.148	1.06

b)

	R_{A-B} (Å)	**$\rho(r_c)$ (e.Å^{-3})**	**$\nabla^2\rho(r_c)$ (e.Å^{-5})**	**λ_1 (e.Å^{-5})**	**λ_2 (e.Å^{-5})**	**λ_3 (e.Å^{-5})**	**$\lvert\lambda_1\rvert/\lambda_3$**	**ε**
C-C								
C_1-C_2	1.398	2.126	-21.282	-16.587	-12.467	7.772	2.134	0.33
C_2-C_3	1.410	2.081	-20.580	-16.142	-12.428	7.990	2.020	0.30
C_3-C_1	1.534	1.703	-14.736	-12.359	-11.424	9.047	1.366	0.08
C-O								
C_1-O_1	1.267	2.414	-0.753	-20.362	-20.199	39.806	0.512	0.01
C_2-O_2	1.378	1.864	-7.774	-12.877	-12.178	17.281	0.745	0.06
C_3-O_3	1.255	2.474	1.803	-21.214	-21.121	44.137	0.481	0.00
C_4-O_2	1.430	1.645	-8.963	-10.143	-9.959	11.139	0.911	0.02
C-H								
C_4-H_{4a}	1.089	1.942	-25.793	-19.136	-18.305	11.648	1.643	0.05

C_4-H_{4b}	1.093	1.912	-24.626	-18.577	-17.714	11.665	1.593	0.05
C_4-H_{4c}	1.094	1.910	-24.557	-18.537	-17.659	11.639	1.593	0.05
O-H								
O_{W1}-H_{1a}	0.989	2.220	-46.467	-42.043	-41.264	36.842	1.141	0.02
O_{W1}-H_{1b}	0.982	2.272	-47.947	-42.973	-42.199	37.225	1.154	0.02
O_{W2}-H_{2a}	0.980	2.291	-48.701	-43.648	-42.672	37.618	1.160	0.02
O_{W2}-H_{2b}’	0.971	2.383	-49.672	-44.127	-43.113	37.568	1.175	0.02
O···H–C^{methyl}								
O_{W2}···H_{4a}-C_4 (HB1)	2.707	0.044	0.578	-0.136	-0.127	0.842	0.162	0.07
O_{W2}···H_{4c}-C_4 (HB2)	3.219	0.015	0.228	-0.036	-0.017	0.281	0.128	0.02
O…H–O								
O_1···H_{2b}’-O_{W2} (HB3)	1.983	0.155	1.633	-0.701	-0.650	2.984	0.235	0.08
O_1···H_{1b}-O_{W1} (HB4)	1.787	0.237	2.548	-1.281	-1.234	5.063	0.253	0.04
O_3···H_{1a}-O_{W1} (HB5)	1.714	0.283	3.068	-1.666	-1.623	6.357	0.262	0.03
O_{W1}···H_{2a}-O_{W2} (HB6)	1.789	0.247	2.655	-1.335	-1.253	5.243	0.255	0.07
C···H-C								
C_2···H_{4a}-C_4	2.771	0.051	0.523	-0.154	-0.109	0.785	0.196	0.05
Li···O								
Li···O_1	2.156	0.110	2.451	-0.570	-0.487	3.509	0.163	0.17
Li···O_2	2.382	0.054	1.257	-0.260	-0.168	1.684	0.154	0.55
Li···O_3	2.053	0.140	3.319	-0.787	-0.754	4.859	0.162	0.04
Li···O_{W1}	2.021	0.159	3.728	-0.955	-0.912	5.595	0.171	0.05
Li···O_{W2}	1.940	0.176	4.747	-1.122	-1.038	6.907	0.162	0.08
Li···C								
Li···C_3	2.860	0.141	3.319	-0.787	-0.754	4.859	0.162	0.04
O···O								
O_2···O_3	2.913	0.062	0.784	-0.173	-0.149	1.105	0.157	0.17
O_2···O_{W1}	2.946	0.068	0.849	-0.195	-0.131	1.175	0.166	0.49
O_1···O_{W1}	3.099	0.053	0.648	-0.148	-0.057	0.854	0.173	1.58

Table S4. Positions of all hydrogen atoms in the α-form, determined by X-ray diffraction (red) and by our dispersion corrected density functional computations (blue) within the corr-B3PW91-D*_0.52 method.

Atom label	Fractional position		
H_2O	x	y	z
H_{W4b}	0.2997	0.6410	0.9384
H_{W4b}	0.3053	0.6467	0.9364
H_{W4a}	0.2829	0.5350	0.8772
H_{W4a}	0.2777	0.5158	0.8688
H_{W3a}	0.4621	0.4016	0.8863
H_{W3a}	0.4609	0.3914	0.8929
H_{W3b}	0.4324	0.4274	0.7823
H_{W3b}	0.4266	0.4183	0.7700
H_{W2a}	0.7402	0.5350	0.9566
H_{W2a}	0.7388	0.5278	0.9686
H_{W2b}	0.7825	0.5597	0.8794
H_{W2b}	0.7831	0.5417	0.8671
H_{W1a}	0.9610	0.4110	0.8928
H_{W1a}	0.9657	0.4022	0.8961
H_{W1b}	0.9435	0.4307	0.7857
H_{W1b}	0.9395	0.4321	0.7749
CH_3			
H_{2b}	0.2922	0.7500	0.5826
H_{2b}	0.2932	0.7626	0.5785
H_{3b}	0.3128	0.7576	0.707
H_{3b}	0.3145	0.7626	0.7173
H_{1b}	0.2665	0.6122	0.6437
H_{1b}	0.2530	0.6084	0.6409
H_{2a}	0.7890	0.7448	0.5966
H_{2a}	0.7895	0.7707	0.6002
H_{3a}	0.7738	0.6047	0.6526
H_{3a}	0.7591	0.5992	0.6454
H_{1a}	0.8218	0.7477	0.7207
H_{1a}	0.8217	0.7380	0.7367

Table S5. Positions of all hydrogen atoms in the β–form, determined by X-ray diffraction (red) and by our dispersion corrected density functional computations (blue) within the corr-B3PW91-D*_0.36 method.

Atom label	Fractional position		
CH_3	x	y	z
H_{4a}	0.588(4)	0.751(3)	0.2134(19)
H_{4a}	0.59916	0.77012	0.23155
H_{4b}	0.612(5)	0.897(3)	0.1454(19)
H_{4b}	0.62387	0.90652	0.14093
H_{4c}	0.514(4)	0.756(3)	0.088(2)
H_{4c}	0.50779	0.73748	0.09719
H_2O			
H_{1a}	0.406(4)	0.065(2)	0.2817(18)
H_{1a}	0.37713	0.08007	0.27888
H_{1b}	0.460(4)	0.093(2)	0.3930(18)
H_{1b}	0.43992	0.10704	0.3995
H_{2a}	0.328(7)	0.544(4)	0.863(3)
H_{2a}	0.28861	0.53516	0.86204
$H_{2b'}$	0.343(13)	0.664(8)	0.921(6)
$H_{2b'}$	0.33502	0.66365	0.93012

References

1. P. E. Blöchl, *Phys. Rev. B*, 1994, **50**, 17953-17979.
2. H. J. Monkhorst and J. D. Pack, *Phys. Rev. B*, 1976, **13**, 5188-5192.
3. S. Grimme, *J. Comput. Chem.*, 2006, **27**, 1787-1799.
4. A.-L. Barrès, J. Geng, G. Bonnard, S. Renault, S. Gottis, O. Mentré, C. Frayret, F. Dolhem and P. Poizot, *Chem. Eur. J.*, 2012, **18**, 8800-8812.
5. C. Frayret, E. I. Izgorodina, D. R. MacFarlane, A. Villesuzanne, A.-L. Barrès, O. Politano, D. Rebeix and P. Poizot, *Phys. Chem. Chem. Phys.*, 2012, **14**, 11398-11412.
6. B. Civalleri, C. M. Zicovich-Wilson, L. Valenzano and P. Ugliengo, *CrystEngComm*, 2008, **10**, 405-410.
7. P. Ugliengo, C. M. Zicovich-Wilson, S. Tosoni and B. Civalleri, *J. Mater. Chem.*, 2009, **19**, 2564-2572.
8. R. Dovesi, R. Orlando, B. Civalleri, C. Roetti, V. R. Saunders and C. M. Zicovich-Wilson, *Z. Kristall.*, 2005, **220**, 571-573.
9. R. Dovesi, V. R. Saunders, C. Roetti, R. Orlando, C. M. Zicovich-Wilson, P. F, B. Civalleri, K. Doll, N. M. Harrison, I. J. Bush, P. D'Arco and M. Llunell, University of Torino, Torino, 2009.
10. A. D. Becke, *J. Chem. Phys.*, 1993, **98**, 5648-5652.
11. W. J. Hehre, R. Ditchfield and J. A. Pople, *J. Chem. Phys.*, 1972, **56**, 2257-2261.
12. D. Feller, *J. Comput. Chem.*, 1996, **17**, 1571-1586.
13. K. L. Schuchardt, B. T. Didier, T. Elsethagen, L. Sun, V. Gurumoorthi, J. Chase, J. Li and T. L. Windus, *J. Chem. Inf. Model.*, 2007, **47**, 1045-1052.